Pergamon

CEMENT AND CONCRETE RESEARCH

Cement and Concrete Research 29 (1999) 143–149

Hydration and temperature development of concrete made with blast-furnace slag cement

Geert De Schutter *

Magnel Laboratory for Concrete Research, University of Ghent, Technologiepark Zwijnaarde 9, B-9052, Ghent, Belgium

Manuscript received 30 October 1998; accepted manuscript 14 November 1998

Abstract

In Europe, massive concrete elements often are made with blast-furnace slag cements. To better deal with the problem of early-age thermal cracking in these cases, a new hydration model for blast-furnace slag cements is developed, which is based on isothermal and adiabatic hydration tests. In the hydration model, the heat production rate is calculated as a function of the degree of hydration and the temperature. The accuracy of temperature simulations using this new hydration model is evaluated by tests on hardening massive concrete cylinders made with blast-furnace slag cement.

Keywords: Blast-furnace slag cement; Hydration; Heat of hydration; Temperature development; Degree of hydration; Temperature

Concrete armour units, used in the armour layer of breakwaters, tend to be massive because of the requirements for hydraulic stability. For example, plain concrete blocks of 30t (Zeebrugge, Belgium), 90t (repair works Sines west breakwater, Portugal), and 150t (repair works Bilbao breakwater, Spain) found application. History has shown that the reliability of rubble mound breakwaters depends not only on hydraulic stability, but also to a large extent on the strength of the armour unit as well [1]. A major problem in this respect is early-age thermal cracking, which leads to reduced quality and durability of the concrete armour unit [2]. These cracks are due to the temperature gradients caused by the heat of hydration of the cement.

In Europe, massive concrete armour units as well as other massive concrete elements such as tunnels, locks, and quay walls, often are made with blast-furnace slag cements. To manage more adequately the problem of early-age thermal cracking in these cases, a general hydration model for blended cements is needed, which enables more accurate temperature simulations during hardening.

1. Experimental program

1.1. Blast-furnace slag cement

The cement considered here is blast-furnace slag cement composed of Portland clincker and ground granulated blast-furnace slag (GGBFS). Two different cements were tested: CEM III/B 32.5 (65 to 80% GGBFS and 35 to 20% Portland clincker) and CEM III/C 32.5 (80 to 95% GGBFS and 20 to 5% Portland clincker). The value of 32.5 refers to the minimal normalised mortar strength at 28 days, expressed in N/mm^2. The chemical composition and the fineness of the cements is given in Table 1.

1.2. Isothermal hydration tests

Isothermal hydration tests were performed using the conduction method (Belgian Standard NBN B12-213) on cement paste with water-to-cement:0.5. Measurement of the heat production rate q (in J/gh) proceeds continuously starting immediately after water addition. This enables registration of the first so-called “wetting” peak of the heat production, i.e., the peak occurring in the first minutes after water addition [3]. However, in the interpretation of the test results (see later), this peak is not considered because of measuring difficulties caused by very small temperature differences between the cement paste and the water bath at the beginning of the test. Furthermore, the integrated contribution of the first peak (total heat Q in J/g) only amounts to a few percent of Q_{max}. Finally, as in practice, concrete is not cast immediately after water addition; the heat corresponding with the first peak is never produced inside the concrete element. The effect of the first peak could be compared to the added mechanical energy due to mixing and is considered implicitly in the casting temperature of the concrete.

* Tel.: 329 264 5521; Fax: 329 264 5845; E-mail: Geert.DeSchutter@eng.ac.be.

0008-8846/99/$–see front matter
PII: S0008-8846(98)00229-4

Table 1
Chemical composition (in %) and fineness

	CEM III/B 32.5	CEM III/C 32.5
SiO_2	26.76	27.12
Al_2O_3	7.33	9.40
Fe_2O_3	2.52	1.63
CaO	50.54	42.95
MgO	5.61	7.23
Blaine (cm^2/g)	4380	4500

Isothermal hydration tests were performed on blast-furnace slag cements CEM III/B 32.5 and CEM III/C 32.5, at three different temperatures (5°C, 20°C, and 35°C).

1.3. Adiabatic hydration tests

With adiabatic hydration tests the heat production rate q can be calculated by measuring the temperature rise of the perfectly insulated concrete, as a function of time. A new adiabatic test method was developed (Fig. 1). Around a cylindrical concrete specimen (diameter 280 mm, height 400 mm) a water ring is created. By a differential thermostat

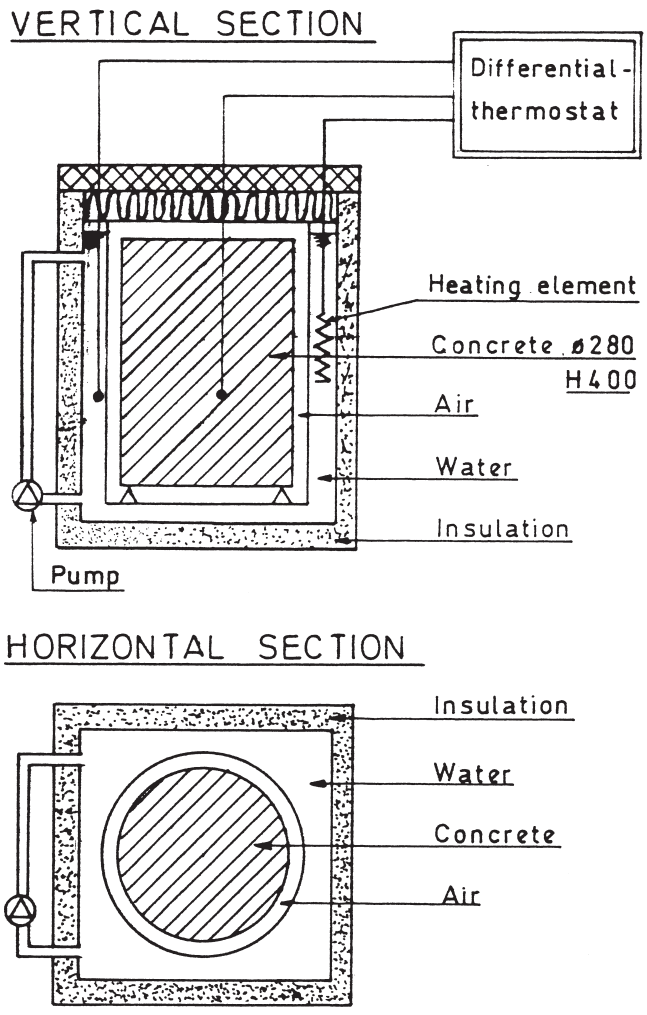

Fig. 1. New adiabatic test methods.

Table 2
Concrete properties

	CEM III/B 32.5	CEM III/C 32.5
Fresh concrete		
Slump (mm)	38	35
Flow (−)	1.43	1.47
Density (kg/m^3)	2420	2400
Hardened concrete (cubes 158 mm)		
Density (kg/m^3)	2380	2360
Mean cube strength at 28 days (N/mm^2)	39.7	20.4

connected with a heating element, the water ring is kept at the same temperature as the concrete. In this way the concrete is maintained in adiabatic conditions. Although theoretically there is no need to place insulation between concrete and water, preliminary experiments indicate that for practical reasons it is a necessity. An air ring seemed to be the ideal solution, because of its high insulating value and its small specific heat. Adiabatic hydration tests were performed on concrete consisting of 300 kg of cement, 150 kg of water, 670 kg of sand, and 1280 kg of gravel. Some characteristics of the fresh and hardened concrete are listed in Table 2.

1.4. Test on massive hardening concrete cylinders

To verify the hydration model developed (see later), massive hardening concrete cylinders with diameter 600 mm and height 1200 mm were tested, using a test set-up as shown in Fig. 2. The bottom and top surfaces of the cylinder were insulated to obtain a radial heat flow, which allows faster and simpler numerical simulation. Around the concrete element an air ring was provided. In this ring, a wind speed of about 4.5 m/s was obtained using a blower. The air temperature varied stepwise with time.

2. Results and discussion

2.1. Degree of hydration and degree of reaction

A fundamental parameter is the degree of hydration α, defined as the cement fraction that has reacted. Due to difficulties in experimentally determining the degree of hydration α, it is often approximated by the degree of heat liberation. As early as the early 1930s, the liberated heat of hydration has been used as an indicator of the degree of hydration [4]. An excellent linear relationship is reported between these tow quantities [4]. Copeland stated that, in view of the theoretical difficulties associated with the definition of the degree of hydration, on the one hand, and the approximate linearity between nonevaporable water content, heat of hydration, and surface area of the cement paste, on the other, any of these quantities can be used as an estimate of the degree of hydration of cement [4]. In the sequel, the de-

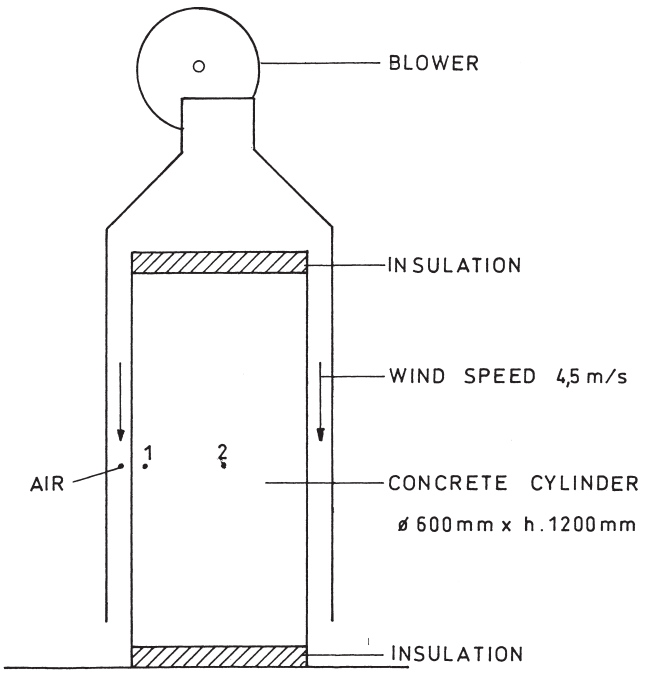

Fig. 2. Test set-up using massive hardening concrete cylinders.

gree of hydration will be calculated as the fraction of the heat of hydration that has been released [Eq. (1)].

$$\alpha(t) = \frac{Q(t)}{Q_{tot}} = \frac{1}{Q_{tot}}\int_0^t q(t)\ dt \quad (1)$$

with α = degree of hydration, t = time, q = heat production rate, Q = cumulated heat of hydration, and Q_{tot} = cumulated heat of hydration at complete hyration.

The total heat of hydration Q_{tot}, liberated after complete hydration, is determined by the cement composition. For Portland cement, Q_{tot} easily can be estimated from the chemical composition by Bogue's formulas, but no equivalent of Bogue's formulas exists for blast-furnace slag cements. Because of this, in the following discussion of the hydration results, we shall work with the degree of reaction r(t), which, in fact, is calculated by the same formula as the degree of hydration [Eq. (1)], but with Q_{tot} replaced by Q_{max}, being the total heat of hydration released at the end of reaction. The relation between degree of hydration α and degree of reaction r is given by Eq. (2):

$$\alpha(t) = r(t) \cdot \alpha_u = r(t) \cdot \frac{Q_{max}}{Q_{tot}}. \quad (2)$$

Depending on the water-to-cement-ratio of the concrete, the end of reaction (degree of reaction r = 1) corresponds with a certain ultimate degree of hydration α_u (e.g., $\alpha_u \approx 0.75$ for water-to-cement ratio ≈ 0.5). For Portland cement the ultimate degree of hydration α_u can be calculated using Mill's formula [4]. For blended cement, no such formula is known. This is a second reason why in the sequel the degree of reaction is used, based on the experimentally obtained value for Q_{max}.

2.2. Hydration model

Fig. 3A shows the isothermal heat production rate q (without first peak) for the cement CEM III/B 32.5. Similar curves were obtained for the cement CEM III/C 32.5, as shown in Fig. 3B. Transferring the time axis t of Fig. 3A into a degree of reaction axis r and standardizing the curves by dividing by the maximum values q_{max} corresponding to each curve, Fig. 4 is obtained. The data used for these calculations are taken from the calorimeter measurements (Fig. 3). Whereas for Portland cement the standardized curves q/q_{max} are independent of the temperature θ [5,6], it seems that for blast-furnace slag cement a single function for describing the effect of the state of the hardening process on the heat production does not exist. The reason can be found in that the hydration of slag cement is composed of two reactions: a Portland reaction (P-reaction) and a slag reaction (S-reaction). The slag mainly is activated by the lime made available during hydration of the Portland cement fraction (and by sulfates and alkalis). From the literature [7,8] it is known that both reactions have different temperature factors. The slag reaction is more sensitive to heat than Portland cement clincker. This follows also from Fig. 4 and explains why a unique, temperature-independent function $q/q_{max}(r)$ does not exist for slag cement.

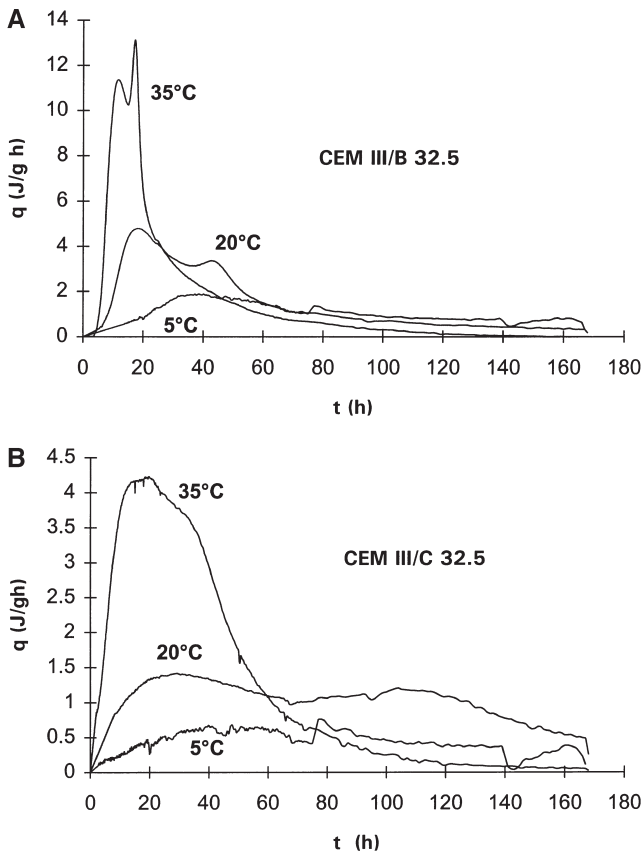

Fig. 3. (A) Heat production rate of CEM III/B 32.5. (B) Heat production rate of CEM III/C 32.5.

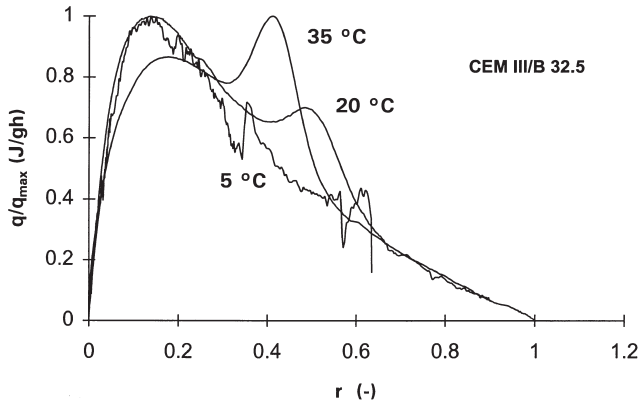

Fig. 4. Standardized curves for CEM III/B 32.5.

A new approach for dealing with this problem is based on the twofold character of the hydration reaction of slag cement: P-reaction and S-reaction. It is assumed that, for the heat production rate q, a superposition is possible of the P- and S-reactions. As indicated in Fig. 5, the heat production of the slag cement can be divided in two separate contributions, corresponding to the P- and S-reactions. Applying this superposition principle on the results for the different test temperatures and standardizing the P- and S-reactions separately, Figs. 6A and 6B are obtained.

The standardized curves for the P-reaction are very similar to those traditionally obtained for Portland cement [6]. The curves for the S-reaction seem to be more symmetric and indicate that the S-reaction ends more rapidly. The issue of the chemical reactivity of slag in cement paste during hydration already has been raised by Roy and Idorn [7]. They observed that the transport of water through a blast-furnace slag cement mortar practically comes to a standstill after a certain hardening time. Moreover, the alkalis and lime, released by the residual Portland cement, are retained in the hydration products of the slag fraction and do not seem to contribute to the hydration of the slag [7].

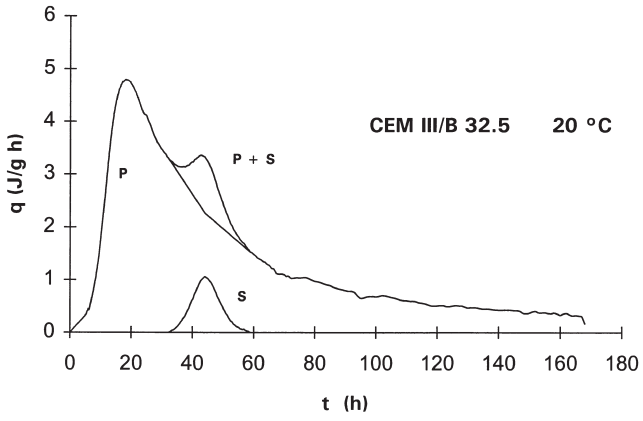

Fig. 5. Superposition of P- and S-reactions.

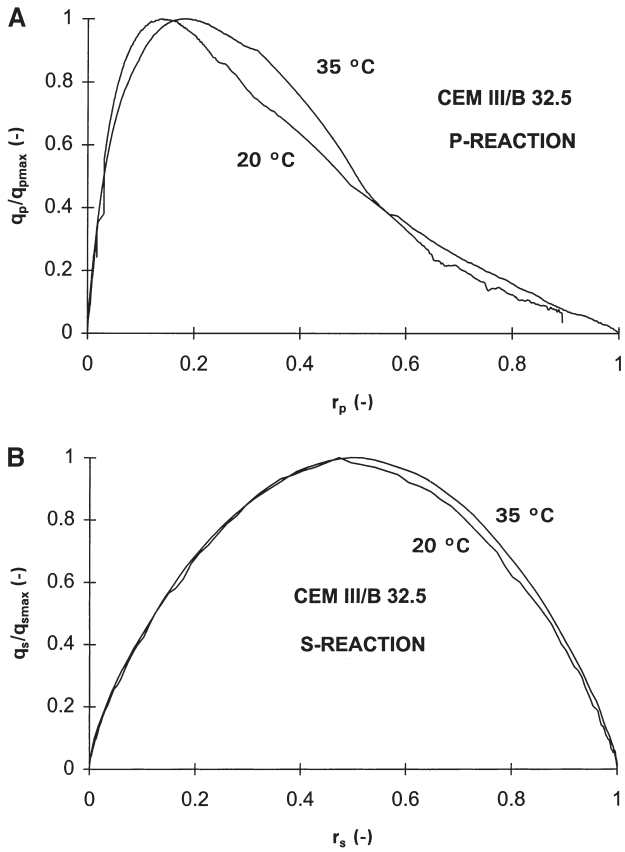

Fig. 6. (A) Standardized P-curves for CEM III/B 32.5. (B) Standardized S-curves for CEM III/B 32.5.

The previous considerations for the slag cement CEM III/B 32.5 lead to a new general hydration model [Eq. (3)] based on the superposition of the heat production of the P- and S-reactions:

$$q = q_P + q_S \tag{3}$$

with q_P = heat production rate of the P-reaction, and q_S = heat production rate of the S-reaction.

For the P-reaction the formulation is very similar to the formulas traditionally given for Portland cement [Eqs. (4–6)] [5,6]:

$$q_P = q_{P,max,20} \cdot f_P(r_P) \cdot g_P(\theta) \tag{4}$$

$$f_P(r_P) = c_P \cdot [\sin(r_P \pi]^{a_P} \cdot \exp(-b_P \cdot r_P) \tag{5}$$

$$g_P(\theta) = \exp\left[\frac{E_P}{R}\left(\frac{1}{293} - \frac{1}{273 + \theta}\right)\right] \tag{6}$$

with $q_{P,max,20}$ = maximum heat production rate of the P-reaction at 20°C, r_P = degree of reaction of the P-reaction, a_P, b_P, and c_P = constants, E_P = apparent activation energy of the P-reaction, R = universal gas constant, and θ = temperature, in °C.

The sine function in Eq. (5) is based on the fact that a maximum value for the heat production rate q_p is reached

somewhere between the zero values at the beginning and end of the P-reaction. The exponential factor results from the general Guldberg and Waage law describing the effect of the concentration of reagents on the rate of corrosion.

The S-reaction can be described mathematically as shown in Eqs. (7–9):

$$q_S = q_{S,max,20} \cdot f_S(r_S) \cdot g_S(\theta) \quad (7)$$

$$f_S(r_S) = [\sin(r_S \pi]^{a_S} \quad (8)$$

$$g_S(\theta) = \exp\left[\frac{E_S}{R}\left(\frac{1}{293} - \frac{1}{273 + \theta}\right)\right] \quad (9)$$

with $q_{S,max,20}$ = maximum heat production rate of the S-reaction at 20°C, r_S = degree of reaction of the S-reaction, a_S = constant, E_S = apparent activation energy of the S-reaction, R = universal gas constant, and θ = temperature, in °C.

The degrees of reaction r_P and r_S can be calculated by means of an expression similar to Eq. (1) as shown in Eqs. (10) and (11):

$$r_P(t) = \frac{Q_P(t)}{Q_{P,max}} = \frac{1}{Q_{P,max}} \int_0^t q_P(t)\, dt \quad (10)$$

$$r_S(t) = \frac{Q_S(t)}{Q_{S,max}} = \frac{1}{Q_{S,max}} \int_0^t q_S(t)\, dt. \quad (11)$$

In these equations $Q_{P,max}$ and $Q_{S,max}$ is the total heat released at the end of P- and S-reactions, respectively. $Q_{P,max}$ and $Q_{S,max}$ can be estimated by integrating the heat production curves obtained from the P- and S-reactions.

As can be seen from Fig. 5, the S-reaction does not start immediately after water addition. The slag hydration only starts in the presence of a certain quantity of alkalis and lime, released by the hydrating Portland clincker. This is implemented mathematically by keeping the second term, q_S, in Eq. (3) equal to zero as long as the degree of reaction of the P-reaction has not reached a threshold value $r_{P,B}$. The parameter $r_{P,B}$ is temperature dependent.

For the moment a linear relationship [Eq. (12)] is applied because of lack of further test results:

$$r_{P,B} = A\theta + B \geq 0 \quad (12)$$

with A and B = constants. A more refined relationship can only be based on a chemical investigation about the nature of $r_{P,B}$.

With an appropriate value of the initial degrees of hydration $r_{P,i}$ and $r_{S,i}$, the induction period of both reactions can be simulated accurately. These initial values also are model parameters, which can be changed to simulate, for example, the effect of retarding agents [9].

Eqs. (3–12) constitute a new general hydration model for blast-furnace slag cements. For the cements CEM III/B 32.5 and CEM III/C 32.5, the values for the different model constants are given in Table 3. The values for the heat production rate and for the cumulative heat of hydration are in good agreement with traditional values found in literature. The apparent activation energy E_p is higher than the value found in literature for Portland cement (33.5) [4]. This might be due to the effect of the slag on the Portland reaction. The different values for E_s for CEM III/B 32.5 and CEM III/C 32.5 can be explained by the fact that, most probably, blast-furnace slags from different sources were used for each cement (different cement manufacturers). No pure slag samples were available to check this.

For now, generalisation of the constants depending on the actual cement composition (slag content, slag properties, chemical composition) is not yet possible.

2.3. Verification by adiabatic test results

Assuming a specific heat equal to 1000 J/kg°C, the curves obtained in the adiabatic hydration tests can be simulated by the hydration model outlined in the previous section. As shown in Fig. 7 simulation and experiment agree very well. The accuracy of the superposition model [Eq. (3)] becomes even clearer when looking at the heat production rate q during the adiabatic hydration test (Fig. 8). The peak corresponding to the slag part of the reaction seems to be simulated in a very accurate way.

Table 3
Model constants

	CEM III/B 32.5	CEM III/C 32.5
a_P (−)	0.667	0.5
b_P (−)	3.5	2.5
c_P (−)	2.8461	2.1425
$q_{P,max,20}$ (J/gh)	4.80	1.42
$Q_{P,max}$ (J/g)	251.0	167.0
E_P (kJ/mol)	45.0	55.0
a_S (−)	0.667	0.667
$q_{S,max,20}$ (J/gh)	1.06	0.62
$Q_{S,max}$ (J/g)	11.3	32.5
E_S (kJ/mol)	80.0	45.0
A (1/°C)	−0.0067	−0.0180
B (−)	0.5133	0.6800
$r_{P,i}$ (−)	0.0001	0.0001
$r_{S,i}$ (−)	0.0001	0.0001

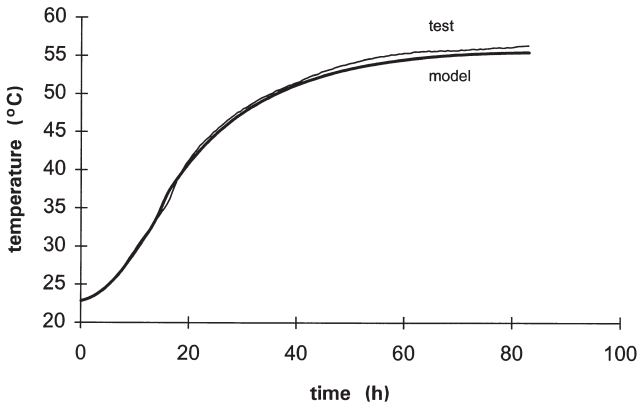

Fig. 7. Adiabatic hydration curve for concrete made with CEM III/B 32.5.

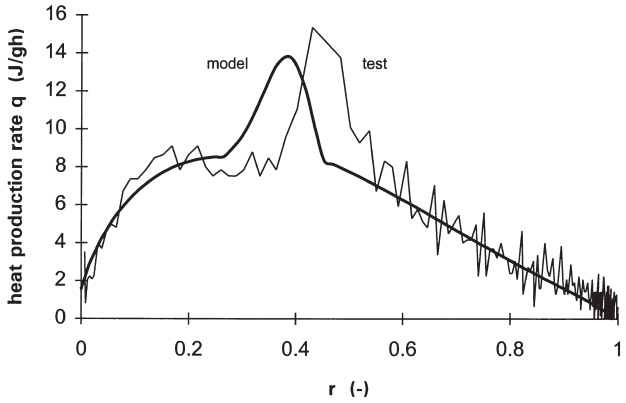

Fig. 8. Heat production rate during adiabatic hydration test.

2.4. Verification by test results obtained on massive cylinders

The temperature field θ(x,y,z,t) in hardening massive concrete elements can be calculated by solving the following boundary value problem [Eqs. (13–15)]:

$$\rho c\frac{\partial\theta}{\partial t} = \frac{\partial}{\partial x}\left(\lambda\frac{\partial\theta}{\partial x}\right)+\frac{\partial}{\partial y}\left(\lambda\frac{\partial\theta}{\partial y}\right)+\frac{\partial}{\partial z}\left(\lambda\frac{\partial\theta}{\partial z}\right)+q,\quad t>0 \qquad (13)$$

$$\theta(x,y,z) = \theta_o,\quad t=0 \qquad (14)$$

$$-\lambda\frac{\partial\theta}{\partial n_i} = h(\theta-\theta_a),\quad t\geq 0 \qquad (15)$$

Eq. (13) is the nonstationary Fourier equation with heat production term q. As the thermal characteristics c (specific heat) and λ (thermal conductivity) depend somewhat on the state of the hardening process [10,11], a time and place dependency is to be considered. The density ρ of the concrete normally remains unchanged in massive elements. Eq. (14) is the initial condition, with θ_0 the temperature of the freshly cast concrete. The boundary condition [Eq. (15)] can be time dependent by using a time-dependent convection coefficient h or a time-dependent environmental temperature θ_a. The boundary value problem [Eqs. (13–15)] was implemented in a computer program at the University of Ghent.

The accuracy of temperature simulations using the newly developed hydration model can be verified by results of the tests on the massive hardening cylinders. The air temperature varied stepwise in time, as shown in Fig. 9A. In Figure 9B the experimental temperature curve for the concrete made with CEM III/B 32.5 is compared with the numerical simulation. Similar results are obtained for the temperature history on other locations in the concrete cylinder and for the concrete made with CEM III/C 32.5.

From these results, as well as from the simulation of the adiabatic test results, it can be concluded that the newly developed hydration model enables accurate simulation of the temperature field in hardening massive concrete elements made with blast-furnace slag cement.

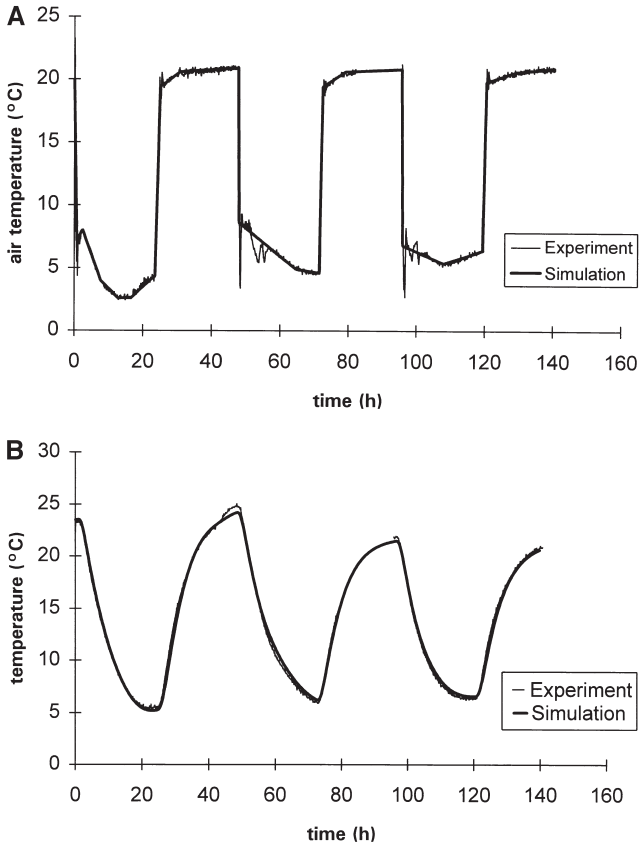

Fig. 9. (A) Air temperature. (B) Concrete temperature at cylinder axis.

3. Conclusion

Based on isothermal and adiabatic hydration tests. a new general hydration model was developed for blast-furnace slag cements. This hydration model, which takes into account the composed character of the cement, enables calculation of the heat production rate as a function of the actual temperature and the degree of hydration. The newly developed hydration model enables accurate simulation of the temperature field in hardening massive concrete elements made with blended cements. This has been verified by temperature measurements on hardening massive concrete cylinders.

References

[1] L. Van Damme, L. Taerwe, R. Dedeyne, J. De Rouck, Quality and durability of concrete armour units, 21st Coastal Engineering Conference, Volume 3, Chapter 156, ASCE, New York, 1988, pp. 2102–2115.

[2] R. Dechaene, J. De Rouck, G. De Schutter, L. Taerwe, F. Van de Weeün, L. Van Damme, Thermal cracking in hardening concrete armour units, PIANC Bulletin, 82 (1994) 61–69.

[3] J. Bensted, Some applications of conduction calorimetry to cement hydration, Adv Cem Res 1 (1) (1987) 33–44.

[4] K. Van Breugel, Simulation of hydration and formation of structure in hardening cement-based materials. PhD Thesis, Technical University Delft, 1991.

[5] H.W. Reinhardt, J. Blauwendraad, J. Jongendijk, Temperature devel-

opment in concrete structures taking account of state dependent properties, International Conference on Concrete at Early Ages, RILEM, Paris, 1982, pp. 211–218.
[6] G. De Schutter, L. Taerwe, General hydration model for portland cement and blast furnace slag cement, Cem Concr Res 25 (3) (1995) 593–604.
[7] D.M. Roy, G.M. Idorn, Hydration, structure and properties of blast furnace slag cements, mortars and concrete, ACI J Nov–Dec (1982) 444–457.
[8] X. Wu, D.M. Roy, C.A. Langton, Early stage hydration of slag cement, Cem Concr Res 13 (1983) 277–286.
[9] G. De Schutter, Influence of retarding agents on the early age thermal cracking behaviour of high performance concrete, 4th International Symposium on Utilization of High-strength/High-performance Concrete, Paris, 1996, pp. 439–447.
[10] G. De Schutter, L. Taerwe, Specific heat and thermal diffusivity of hardening concrete, Mag Concr Res 47 (172) (1995) 203–208.
[11] G. De Schutter, Fundamental and practical study of thermal stresses in hardening massive concrete elements, PhD Thesis, Magnel Laboratory for Concrete Research, University of Ghent, Ghent, 1996.